

Revealing and quantifying the 3D nano- and microscale structures in self-assembled cellulose microfibrils in dispersions

*Srivatssan Mohan,[†] Jissy Jose,^{‡,a} Anke Kuijk,^{‡,b} Sandra J. Veen,^{‡,c} Alfons van Blaaderen,[†] and
Krassimir P. Velikov^{†,‡,§,*}*

[†] Soft Condensed Matter, Debye Institute for NanoMaterials Science, Utrecht University
Princetonplein 5, 3584 CC Utrecht, The Netherlands

[‡] Unilever R&D Vlaardingen, Olivier van Noortlaan 120, 3133 AT Vlaardingen, The
Netherlands.

[§] Institute of Physics, University of Amsterdam, Science Park 904, 1098 XH Amsterdam, The
Netherlands

Corresponding author: krassimir.velikov@unilever.com

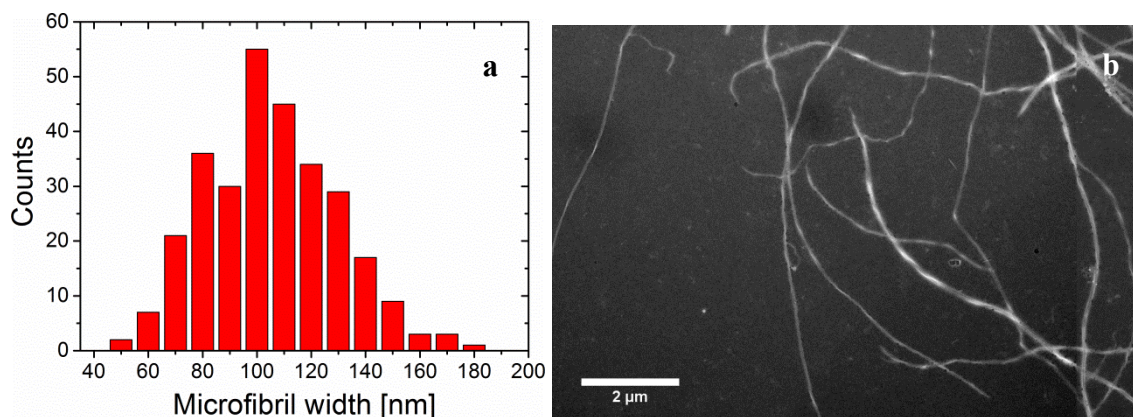


Figure S1: (a) Width distribution of cellulose microfibrils. (b) Representative TEM image (contrast inverted) of CMF.

Note 1 for Figure S1: Nomenclature of cellulose fibrils

The term microfibrils and nanofibrils are used synonymously for cellulose systems¹. These terms, however, are not synonymous to ‘microfibrillated cellulose’ processed from plant sources which can contain a variety of fibrillar fragments of different sizes.² In the case of bacterial cellulose, microfibrils are referred to as the ribbon shaped fibrils formed by aggregation of several ‘elementary fibrils’ of about 5 nm in width. The width of cellulose microfibrils (CMF) sourced from bacteria was reported to be in the range of 70-145 nm.³ Fig. S1a shows the width distribution of dried CMFs analyzed from TEM images. The average width was found to be 95 nm after analyzing about 100 fibrils.

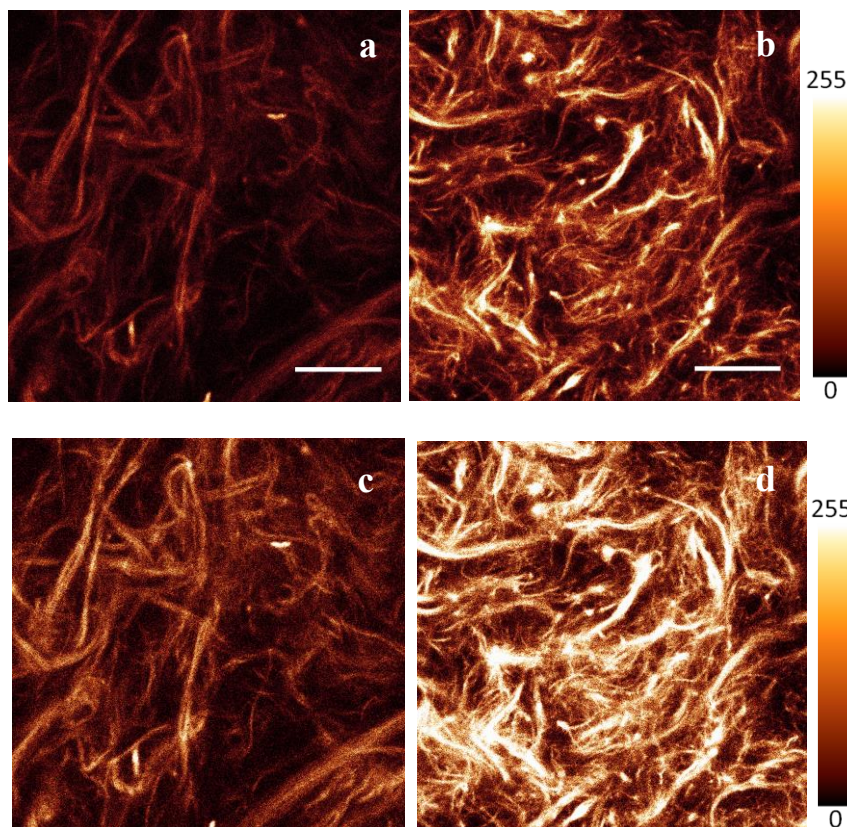


Figure S2. Comparison of (a) non-covalently labelled CMF with Congo red; (b) covalently labelled CMF with FITC; (c) brightness and contrast stretched image (a); (d) brightness and contrast stretched image (b). Scale bars represent 10 μm .

Note 2 for Figure S2: Effect of fluorophore labelling method on imaging cellulose.

An example of different fluorescent labelling methods on CMF is shown in Fig. S2. It was found that the contrast of images of CMF labelled by covalent attachment of FITC was considerably better than non-covalent labelling with Congo red. Both confocal micrographs were taken at same settings, same gain, except that Congo red is excited at 500 nm and FITC at 490 nm wavelength. In order to make the visualization better for comparison, the intensity distribution of both the images were stretched equally up to 50% by increasing the brightness and contrast. Figures S2c and S2d are intensity stretched images of S2a and S2b, respectively. It could be noted that the intensity stretched Congo red dyed image appears more grainy and

also the resolution of fibrils is still not as clear as to that of un-stretched FITC dyed image (Fig. S2b). Therefore, one can conclude from this result that covalent labeling of dye significantly improves the contrast and hence the resolution of fibrils for micro-structural analysis.

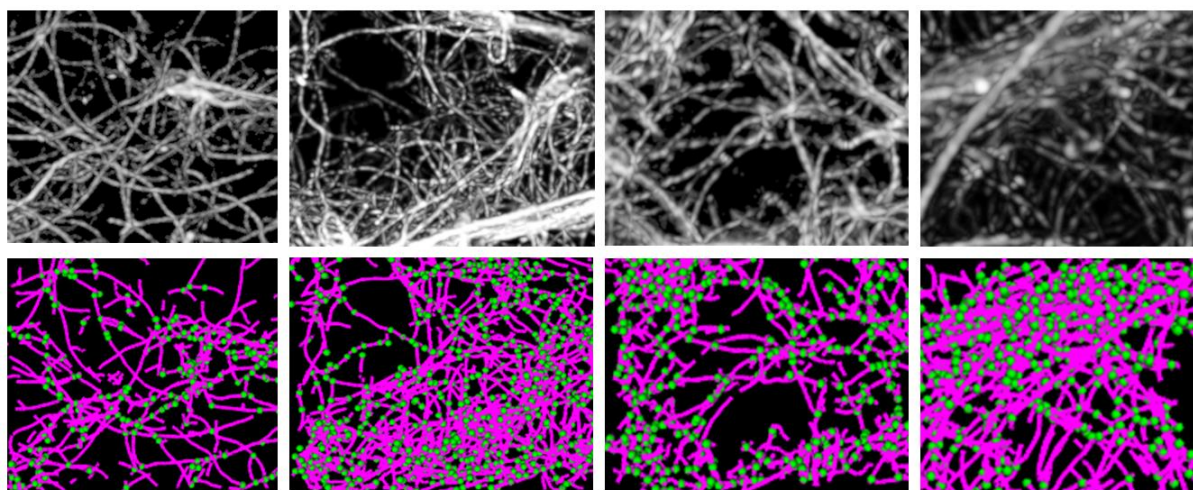


Figure S3. Magnified portions of confocal (top row) and SOAX (bottom row) rendered images of CMF networks from Fig. 2 at different volume fractions (0.11%, 0.13%, 0.18% and 0.22% ϕ from left to right). The green spots correspond to fibril junctions and the purple lines correspond to centerlines of fibril contours.

Note 3 for Figures S3: Comparison of confocal image and its reconstruction.

A series of magnified portions of confocal images in Fig. 2 and its respective SOAX rendered image of the CMF networks at different volume fractions are displayed in Fig. S3, in order to verify the exactness of the image reconstruction process. Overall, it can be observed that the reconstructed images closely resemble the original confocal images. On a closer look, we could identify few drawbacks, mainly the presence of few false positive junctions and that the larger fibril bundles remain unresolved. The reason for this might be that the fibril separation distance might be smaller than the PSF width, in the case of bundles. The junctions are

defined by reconfiguring and clustering local T-junction points that are formed when one Stretching Open Active Contours (SOAC) collides with another SOAC body.⁴ The anisotropy in the point spread function shape may be a contributing factor to the few false junction points arising from fibrils close to each other. However, the periodic intensity variation along the fibril contours does not seem to affect the tracking process unless the intensity is too low to not be accounted by the set ridge threshold parameter. The heterogeneous nature of the networks pose a significant challenge to be reconstructed accurately and the results shown here are as good as we could achieve, with existing image analysis methods.

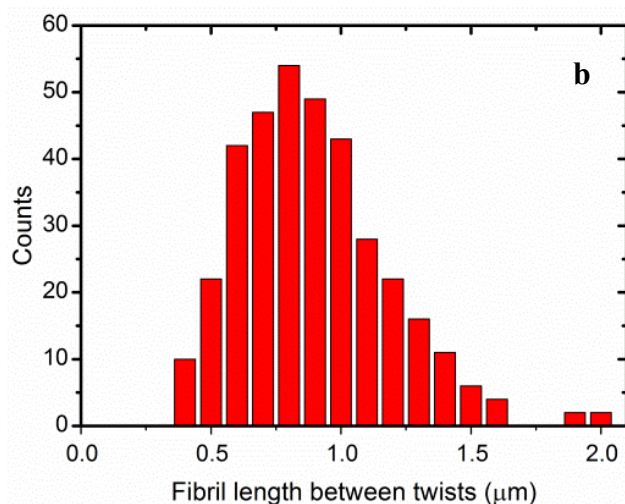
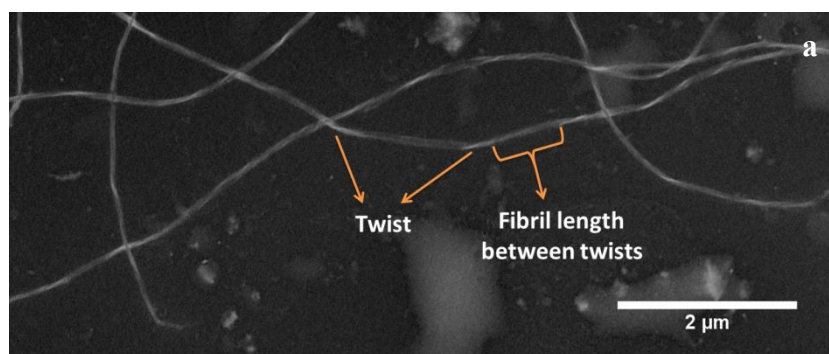


Figure S4. (a) TEM image (inverted contrast) of CMF dried from water dispersion showing twists represented by the brighter segments. (b) Distribution of fibril lengths between twists measured from TEM images.

Note 4 for Figure S4: Transmission Electron Microscopy of cellulose microfibrils and determination of the distribution of fibril lengths between twists in dried state.

In order to compare the fibril lengths between twists in the dispersed or ‘wet’ state with that of in the dried state, transmission electron microscopy (TEM) was performed on fibrils that were dried from a dispersion. We used negatively stained samples of Carboxymethyl cellulose (CMC) adsorbed cellulose microfibrils (1:4=CMC:CMF) dried from water dispersion. TEM was performed on a Tecnai 20 system from FEI. A drop of dispersion was placed on a carbon only 300 mesh copper TEM grid (Agar Scientific), of which the surface was made hydrophilic by glow discharge. Excess solvent was blotted away with a small filter paper, after which the sample was negatively stained by adding a drop of phosphotungsten acid (2% w/v) in water onto the grid. The samples were left to dry in air before imaging. A representative inverted contrast TEM image of CMF is shown in Fig. S4a. The twists are identified with brighter regions along the fibril contour. The lengths of fibrils between subsequent twists were measured using ImageJ 1.49k (Fig. S4a) for about 75 fibrils and the results are plotted as shown in Fig. S4b.

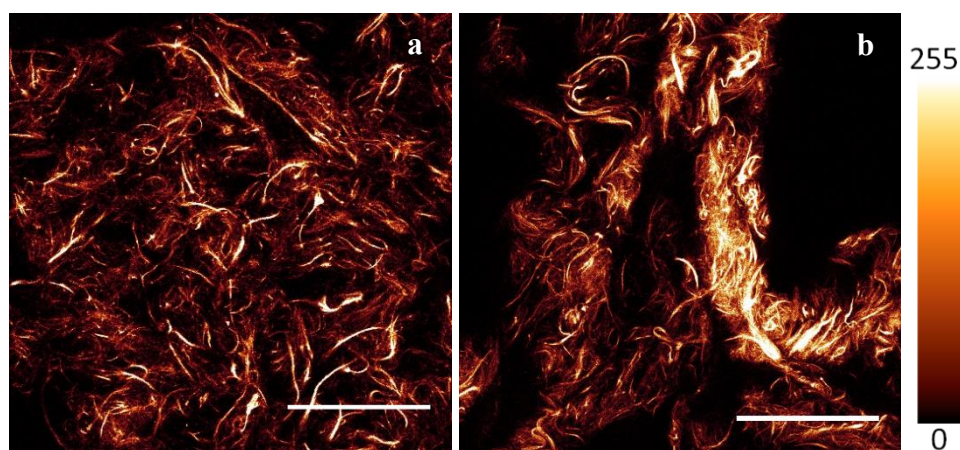


Figure S5. 2D confocal images of CMF from bacterial cellulose (a) before and (b) after a simple shear. Scale bars represent 50 μm.

Note 5 for Figure S5: Observation of changes in CMF network structure on application of shear

In preliminary measurements, we have also observed the effect of simple shear applied on the microstructure of CMF networks using confocal microscopy. Figure S5 shows the marked difference in the microstructure of CMF networks before and after a simple shear (with no control of shear rate) between two cover slips. The formation of higher order aggregates upon shear can be observed clearly. These preliminary investigations indicate the relevance for a more in-depth study of the effects of shear on the microstructure of these networks using a shear cell attached to confocal microscope.

Supporting Movie M1:

The movie (Mohan et al_Supporting movie_M1) shows 0.02% ϕ CMF dispersed in DMSO imaged in resonant scanner mode in reflectance confocal microscope. The network structure is unstable and changes with time due to loss of topological constraints leading to dangling fibrils.

References

1. Siró, I.; Plackett, D., Microfibrillated cellulose and new nanocomposite materials: a review. *Cellulose* **2010**, *17* (3), 459-494.
2. Chinga-Carrasco, G., Cellulose fibres, nanofibrils and microfibrils: The morphological sequence of MFC components from a plant physiology and fibre technology point of view. *Nanoscale Research Letters* **2011**, *6*, 1-7.
3. Fink, H.-P.; Purz, H. J.; Bohn, A.; Kunze, J., Investigation of the supramolecular structure of never dried bacterial cellulose. *Macromol. Symp.* **1997**, *120* (1), 207-217.
4. Xu, T.; Vavylonis, D.; Tsai, F. C.; Koenderink, G. H.; Nie, W.; Yusuf, E.; Lee, I. J.; Wu, J. Q.; Huang, X., SOAX: A software for quantification of 3D biopolymer networks. *Sci. Rep.* **2015**, *5*.